

# Direct Observation of Molecular Orbital Mixing in a Solvated Organometallic Complex\*\*

Edlira Suljoti, Raul Garcia-Diez, Sergey I. Bokarev,\* Kathrin M. Lange, Roland Schoch, Brian Dierker, Marcus Dantz, Kenji Yamamoto, Nicholas Engel, Kaan Atak, Oliver Kühn, Matthias Bauer,\* Jan-Erik Rubensson, and Emad F. Aziz\*

Engineering new materials with novel catalytic properties is a subject of strong technological relevance, while understanding the reaction dynamics, that is, breaking and making chemical bonds as well as the ligand-exchange dynamics, is a subject of scientific investigation. In this context multi-dimensional spectroscopic studies of the electronic and geometric structure of catalysts are emerging as challenging state-of-the-art methods for the fundamental understanding of reaction mechanisms in catalysis. In this framework, X-ray spectroscopy is an important area of synchrotron-based research that probes fundamental properties of matter, while addressing issues related to modern technology.

The combination of X-ray absorption (XA) and resonant inelastic X-ray scattering (RIXS) techniques at the ligand and metal sites can give an atom-specific, chemical-state-selective, crystal-field-symmetry- and orbital-symmetry-resolved description of the electronic structure of catalysts. In the present work, we apply these techniques to study molecular orbital mixing and donation/backdonation in the  $[\text{Fe}(\text{CO})_5]$  complex in solution.

Transition-metal carbonyls play an important role in organometallic photochemistry,<sup>[1]</sup> catalysis,<sup>[2]</sup> and biological processes. Iron–carbonyl complexes, in particular, are used as catalysts in a wide range of chemical reactions and industrial applications,<sup>[3]</sup> such as light-driven hydrogen generation,<sup>[4]</sup> Fischer–Tropsch synthesis,<sup>[2,5]</sup> and catalytic removal of CO from exhaust gases.<sup>[6]</sup> At the core of the functionality of these systems lies the fast electron dynamics and efficient energy transfer between the transition-metal atom and the ligands mediated by the chemical bond, which lead to the fast photodissociation of carbonyl ligands and the high catalytic activity of the fragmented molecules.<sup>[7]</sup> Therefore, a quantitative understanding of the chemical bond in carbonyl complexes is needed in order to design new catalysts with improved activity.

The ligand–metal bonding is usually described in a frontier orbital approach, the so-called  $\sigma$ -donor/ $\pi$ -acceptor mechanism.<sup>[8]</sup> In  $[\text{Fe}(\text{CO})_5]$  the frontier orbitals involved in bonding are the highest occupied molecular orbital (MO),  $5\sigma$ , and the lowest unoccupied molecular orbital,  $2\pi^*$ , of the CO molecule, and the Fe 3d orbitals. A covalent bond between the CO  $5\sigma$  and metal states of  $\sigma$  symmetry is formed, leading to a charge donation to the metal, which is compensated by a backdonation to the CO  $2\pi^*$  orbitals. The charge donation/backdonation mechanism for the iron pentacarbonyl complex

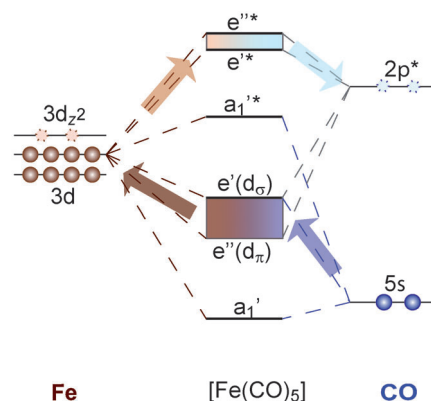


**Figure 1.** Covalency and donation/backdonation in an  $[\text{Fe}(\text{CO})_5]$  molecule: simplified molecular orbital scheme of the frontier orbitals. Charge is donated from a  $5\sigma$  orbital of CO to unoccupied iron 3d orbitals, and backdonated from occupied iron 3d orbitals to the empty  $\pi^*$  CO orbitals. The resulting molecular orbitals have both ligand and metal symmetry contribution. The color code throughout this communication: brown corresponds to iron contributions and blue to CO contributions to MOs.

[\*] Dr. E. Suljoti, R. Garcia-Diez, Dr. K. M. Lange, B. Dierker, M. Dantz, K. Yamamoto, N. Engel, Dr. K. Atak, Prof. Dr. E. F. Aziz  
Joint Ultrafast Dynamics Lab in Solutions and at Interfaces (JULiQ)  
Helmholtz-Zentrum Berlin für Materialien und Energie  
Albert-Einstein-Strasse 15, 12489 Berlin (Germany)  
E-mail: emad.aziz@helmholtz-berlin.de

Prof. Dr. E. F. Aziz

Department of Physics, Freie Universität Berlin  
Arnimallee 14, 14159 Berlin (Germany)

Dr. S. I. Bokarev, Prof. Dr. O. Kühn  
Institut für Physik, Universität Rostock  
Universitätsplatz 3, 18051 Rostock (Germany)  
E-mail: sergey.bokarev@uni-rostock.de

R. Schoch, Prof. Dr. M. Bauer  
Fachbereich Chemie, TU Kaiserslautern  
Erwin-Schrödinger-Strasse 54, 67663 Kaiserslautern (Germany)  
E-mail: bauer@chemie.uni-kl.de

Prof. Dr. J.-E. Rubensson  
Department of Physics and Astronomy, Uppsala University  
Box 516, SE 751 20 Uppsala (Sweden)

[\*\*] We acknowledge support from the staff of the Bessy II facility, Berlin (Germany). This work was supported by the Helmholtz-Gemeinschaft (Young Investigator Fund) and the European Research Council (E.F.A.). Funding by the Carl-Zeiss foundation is also gratefully acknowledged (M.B.).

Supporting information for this article is available on the WWW under <http://dx.doi.org/10.1002/anie.201303310>.

is schematically illustrated in Figure 1. It is desirable to directly measure the strength of donation and backdonation in carbonyl complexes, with a direct probe of the MO composition at different atoms in the complex.<sup>[9]</sup> This element-specific information can be provided by applying resonant X-ray spectroscopy.<sup>[10]</sup> In the X-ray absorption process a spatially localized iron 2p core electron is resonantly excited into an unoccupied valence orbital. The core-excited state is far from energy equilibrium and the core hole will be filled by an electron from an occupied valence orbital. The energy released in this process can be carried by a photon which is emitted, leaving the system in an electron-hole valence-excited state. The process is called resonant X-ray emission or resonant inelastic X-ray scattering (RIXS). Since the transition is governed by the dipole operator, only atom-specific symmetry-allowed valence orbitals are measured, namely the occupied Fe 3d orbitals. Due to hybridization, an empty Fe 2p core hole can be filled by an electron coming from the mixed ligand-metal orbital levels.<sup>[11]</sup> If the excited electron is primarily localized at the Fe site and the hole is primarily localized at the CO oxygen, the RIXS process leads to a “charge-transfer” (CT) excitation.<sup>[12]</sup> The intensity of such a transition directly probes the strength of molecular orbital mixing in the covalent bond. This method has been successfully applied to probe the molecular hybridization in gas molecules adsorbed on different metal surfaces.<sup>[13]</sup> Due to the strong contribution coming from the bulk metal these studies have been restricted to investigate the adsorbed ligands only.

In this study, we apply RIXS on both the metal and the ligands to directly probe the strength of orbital mixing at each atom. The experimental XAS and RIXS findings are augmented by ab initio multiconfigurational calculations based on the multireference first-principles restricted active space self-consistent-field (RASSCF) method combined with state interaction (RASSI) treatment of spin-orbit effects. The details of the experimental and theoretical calculations are given in the Supporting Information. The RASSCF calculations of  $[\text{Fe}(\text{CO})_5]$  reveal a complex multiconfigurational electronic structure of ground and excited valence and core states, but the results can be analyzed in a straightforward fashion with the MOs presented in Table S1 and schematically depicted in Figure 1. The CO 5 $\sigma$  orbital makes bonding ( $\alpha_1'$ ) and anti-

bonding ( $\alpha_1'^*$ ) combinations with the Fe 3d orbitals. The first one is occupied and has mainly CO 5 $\sigma$  character, while the second one has notable Fe 3d character (Table S1). The CO 2 $\pi^*$  orbital makes bonding ( $e', e''$ ) and antibonding ( $e'^*, e''^*$ ) combinations with the Fe 3d orbitals of  $\sigma$  ( $e'(d_{\sigma}), e'^*$ ) and ( $e''(d_{\pi}), e''^*$ ) symmetry. The bonding orbitals are occupied and have primarily Fe 3d character, whereas the antibonding orbitals are unoccupied and are dominated by CO 2 $\pi^*$  character (Table S1). Based on these results the spectral features at the iron  $L_{2,3}$ -edge XAS, (Figure 2a) are assigned to excitation of the 2p electron into the antibonding orbitals. The pre-peak located at 708.6 eV is due to excitation to two states: 1) to  $\alpha_1'^*$  and 2) to  $\alpha_1'^*$  with a small contribution of  $e''^*$ , while the main peak located at 710.6 eV consists of several states but the strongest one are 3) almost equal contributions of  $\alpha_1'^*$ ,  $e'^*$ , and  $e''^*$  states, and 4)  $e'^*$  with admixture of  $e''^*$ . A broadened replica of these features is found at higher energies at the  $L_2$ -edge due to the shorter core-hole lifetime caused by the fast Coster–Kroenig decay process. The theoretical and experimental X-ray absorption spectra in Figure 2a agree very well. Tuning the excitation across the  $L_3$ -edge we observe several RIXS features (Figure 2b) that are satisfactorily reproduced by ab initio calculations (Figure 2c). The feature coinciding with the excitation energy (highlighted in yellow) is assigned to Thomson scattering and resonant elastic X-ray scattering (participator channel), where the excited electron recombines with the core hole, leaving the system in the ground state. The emission band highlighted in brown and

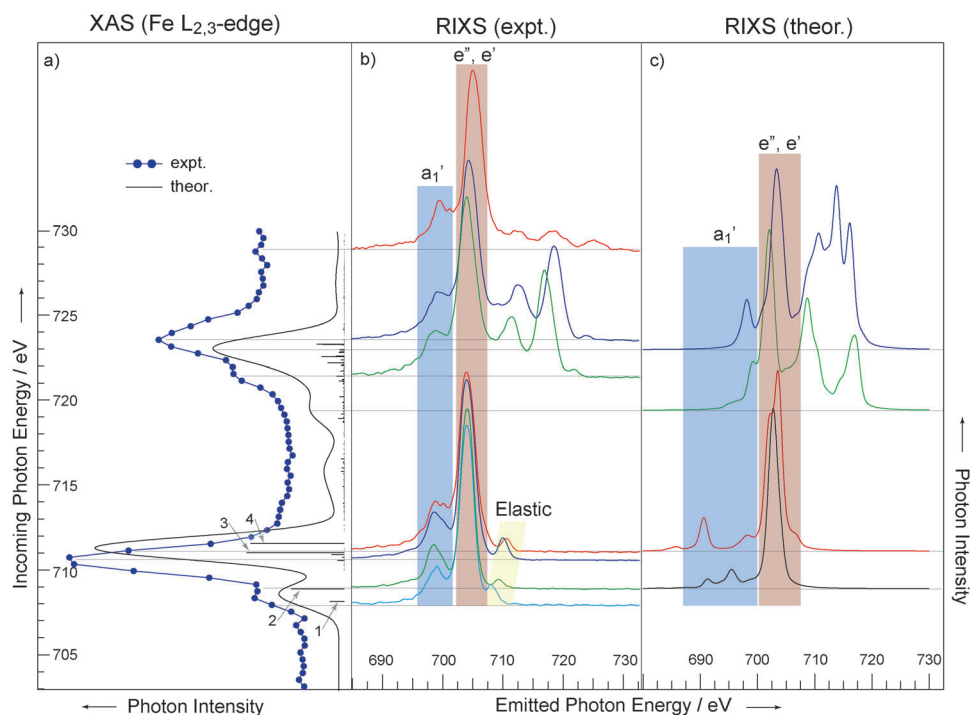


**Figure 2.** Experimental and theoretical XAS and RIXS spectra of the Fe  $L_{2,3}$ -edge. a) Experimental (blue dots) and calculated (black solid line and bars)  $L_{2,3}$ -edge XAS spectra of iron. The dominating character of the probed orbitals is assigned for the spectral features at the  $L_3$ -edge. A series of RIXS experimental (b) and theoretical (c) spectra measured across the Fe  $L_3$ - and  $L_2$ -edges. The dominating characters of the RIXS final states are assigned. Scattering to the same final states is highlighted with the same color. In the theoretical spectra the elastic peak is excluded.

located at around 705 eV is due to the filling of the  $2p_{3/2}$  core hole with an electron coming from the  $e'(d_o)$ , and  $e''(d_\pi)$  occupied states. Since these states have mainly Fe 3d character, the second step of the RIXS process is primarily a local atomic transition due to  $e', e'' \rightarrow a_1^*$  final state excitations, corresponding to local  $d \rightarrow d$  excitations. The lack of dispersion of the 705 eV peak suggests that the excited electron couples little at the iron site, making the second step of the RIXS process fairly independent of the excitation energy. This supports strong ligand-metal orbital mixing and a large spatial delocalization of the MOs. The blue-highlighted RIXS band in Figure 2b is due to the filling of the  $2p_{3/2}$  core hole by an electron coming from the  $a_1'$  valence orbital. The agreement between experiment and theory for this transition is not perfect, which can be traced to the fact that the RASSCF method includes only part of the electron correlation. The  $a_1'$  state has 81 % CO  $5\sigma$  character and is only weakly mixed with Fe 3d character; therefore the second step of the RIXS process transfers electrons from the ligand to the metal. The intensity of this transition is proportional to the ligand-to-metal charge donation. The relative strong intensity observed in the experimental spectra is indicative of a strong MO mixing and a strong  $\sigma$  covalent bond, as predicted by theory (Table S1). Tuning the excitation at the  $L_2$ -edge we observe two additional RIXS bands located between 710 eV and 722 eV. Theoretical calculations show that the character of these two bands is more complex in nature. Similar to  $L_3$ -edge excitation, the two bands are due to  $e', e'' \rightarrow a_1^*$  (local  $d \rightarrow d$ ) and  $a_1' \rightarrow a_1^*$  (charge-transfer) excitations additionally mixed with shake-up and shake-off excitations. The measured intensity of these two transitions in the experimental spectra is smaller than in the calculated ones, addressing a strong (nonradiative) Coster-Kronig decay process at the  $L_2$ -edge.

In order to probe the backdonation in the metal-ligand bond we performed XAS and RIXS experiments at the oxygen K-edge of the carbonyl ligands. The experimental results and theoretical spectra are shown in Figure 3 a–c. The XAS spectrum is dominated by one strong resonance located at 534.4 eV which is assigned to excitations from the O 1s orbital to the  $a_1^*$  MO, for the pre-edge region, and to CO  $2\pi^*$ -dominated  $e'^*$  and  $e''^*$  orbitals, for the main-edge region (Figure 1a). The XAS peak position is very close to the corresponding resonance energy in free CO (534.2 eV). The RIXS spectra together with the radiative processes following the resonant excitation are shown in Figure 3 b,c. The main contributions to the spectra are given by the occupied  $4\sigma$  and

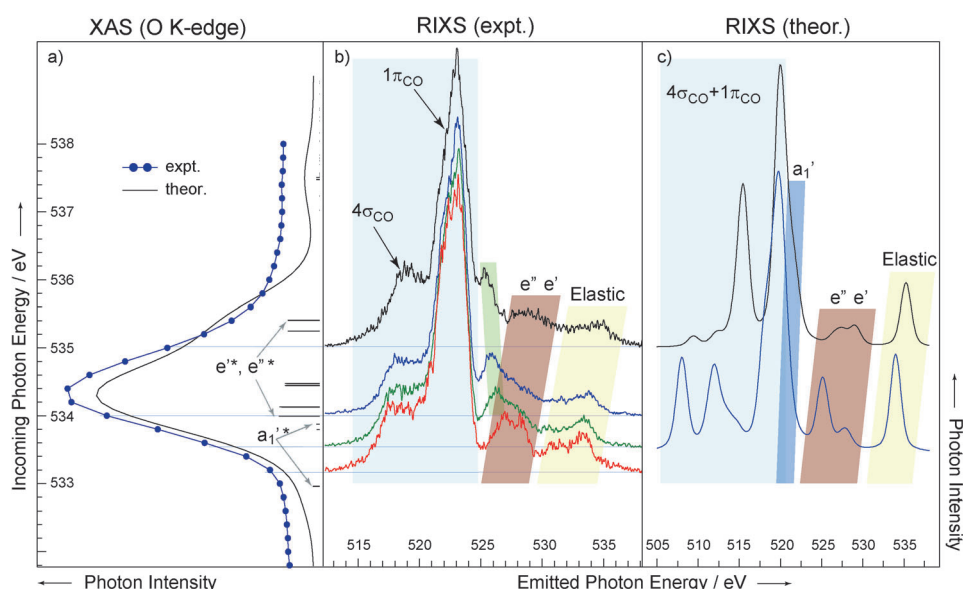


**Figure 3.** Experimental and theoretical XAS and RIXS spectra of the oxygen K-edge. a) Experimental (blue dots) and calculated (black solid line and bars) K-edge XAS spectra of oxygen. A series of RIXS experimental (b) and theoretical (c) spectra across the oxygen K-edge. The dominating characters of the final states are assigned. Scattering to the same final states is highlighted with the same color.

$1\pi$  CO valence orbitals, located at around 518 eV and 522 eV, respectively (highlighted in blue in Figure 3b,c). Again, for the reason mentioned above, the agreement between experiment and theory is not exceptional for the  $4\sigma$  transition. At the high-energy end of the spectra (highlighted in yellow) the elastic peak, associated with the recombination of the excited electron and the core hole, is located. The structure of this band in the experimental spectrum is due to vibrational excitations<sup>[14]</sup> in the electronic ground state, and the intensity distribution reflects the nuclear dynamics in the intermediate state as well as the ground-state potential energy surface. The similarity with the gas-phase spectra<sup>[14]</sup> suggests that it is primarily the CO stretch which is excited in the electronic ground state. The present theoretical model does not include vibrational effects and therefore cannot reproduce a possible vibronic structure of RIXS peaks. In between the participator and CO  $1\pi$  band, the charge-transfer transitions are observed (highlighted in brown in Figure 1b,c). According to theory, they are assigned to transitions where the O 1s hole is filled by electrons from the Fe 3d-dominated  $e'(d_o)$  and  $e''(d_\pi)$  orbitals, thus populating  $e', e'' \rightarrow e'^*, e''^*$  final states, corresponding to metal-to-ligand charge transfer. As the excitation energy is tuned over the resonance, the maximum of the charge-transfer band disperses toward low emission energies, converging to the CO  $a_1'$  molecular state (highlighted in Figure 3b). The local energy conservation in the RIXS process predicts Raman dispersion of the band to higher emission energies (Figure 1c). Most probably the energy losses of this band are due to the nuclear dynamics in the intermediate state. It is well-known that detuning below the resonance leads to shortened effective RIXS duration time,<sup>[10a]</sup> so that the influence of the nuclear dynamics in the intermediate state becomes smaller. This is in line with the observation of the sharpest features at energies just before the XAS

resonance. Tuning the excitation to the resonance, the RIXS duration time becomes longer and therefore the vibrational dynamics in the intermediate state has a larger influence on the spectral shapes. Indeed, the energy losses in the charge-transfer process are due to excitation of the Fe 3d-dominated  $e'(d_\sigma)$  and  $e''(d_\pi)$  electrons to the antibonding CO-dominated  $e'^*$  and  $e''^*$  orbitals. Therefore the metal–ligand bond is elongated and weakened in the intermediate state, and the complex may even move towards dissociation and release of free CO molecules. This could be the reason why the charge-transfer band in the experimental spectra converges towards the  $\alpha'_1$  molecular state, which consists mainly of CO character. Time-of-flight<sup>[7a]</sup> and electron-diffraction experiments<sup>[7b]</sup> have indeed reported the ultrafast (ca. 100 fs) dissociation of  $[\text{Fe}(\text{CO})_5]$  molecule to  $\{\text{Fe}(\text{CO})_4\}$  and  $\{\text{Fe}(\text{CO})_3\}$  fragments upon photo-excitation of the catalyst. The observation of high energy losses in the metal-to-ligand charge-transfer band clearly indicates a dissociative final state corresponding to dissociation prior to the core-hole decay. This is evidence that the early dynamics of  $[\text{Fe}(\text{CO})_5]$  photodissociation starts at much shorter times than already reported.<sup>[7]</sup>

In conclusion, we employed a multidisciplinary approach involving chemistry, physics, and computational modeling to challenge the fundamental understanding of the electronic structure of the ironpentacarbonyl complex under catalytically relevant in situ conditions. These studies showed that the RIXS method combined with elaborated ab initio multi-configurational theory facilitates the probing of the orbital mixing and the strength of charge donation/backdonation in complex organometallic systems at the atomic level under realistic conditions. Therefore, the RIXS method can be a very useful tool for application to “bond-selective chemistry”, the ultimate challenge in chemical reactions and catalysis. The present work can contribute to a better understanding of reaction dynamics at ultrafast timescales related to metal–ligand–solvent interactions. These insights may lead to improved control of catalytic properties and may have a significant impact on the engineering of new advanced catalytic materials.

Received: April 19, 2013

Published online: July 23, 2013

**Keywords:** backdonation · organometallic complexes · resonant inelastic X-ray scattering · X-ray spectroscopy

- [1] G. L. Geoffroy, M. S. Wrighton, *Organometallic photochemistry*, Academic Press, New York, **1979**.
- [2] J. L. Casci, C. M. Lok, M. D. Shannon, *Catal. Today* **2009**, *145*, 38–44.
- [3] a) T. D. Walter, S. M. Casey, M. T. Klein, H. C. Foley, *Energy Fuels* **1994**, *8*, 470–473; b) A. D. King, R. B. King, D. B. Yang, *J. Am. Chem. Soc.* **1980**, *102*, 1028–1032.
- [4] F. Gärtner, B. Sundararaju, A.-E. Surkus, A. Boddien, B. Loges, H. Junge, P. H. Dixneuf, M. Beller, *Angew. Chem.* **2009**, *121*, 10147–10150; *Angew. Chem. Int. Ed.* **2009**, *48*, 9962–9965.
- [5] B. Cornils, W. A. Herrmann, M. Rasch, *Angew. Chem.* **1994**, *106*, 2219–2238; *Angew. Chem. Int. Ed. Engl.* **1994**, *33*, 2144–2163.
- [6] S. Kureti, W. Weisweiler, K. Hizbullah, *Appl. Catal. B* **2003**, *43*, 281–291.
- [7] a) L. Banares, T. Baumert, M. Bergt, B. Kiefer, G. Gerber, *Chem. Phys. Lett.* **1997**, *267*, 141–148; b) H. Ihee, J. M. Cao, A. H. Zewail, *Angew. Chem.* **2001**, *113*, 1580; *Angew. Chem. Int. Ed.* **2001**, *40*, 1532.
- [8] J. Chatt, L. A. Duncanson, *J. Chem. Soc.* **1953**, 2939–2947.
- [9] A. P. Hitchcock, *Phys. Scr.* **1990**, *T31*, 159–170.
- [10] a) F. Gel'mukhanov, H. Agren, *Phys. Rep.* **1999**, *312*, 87–330; b) O. Karis, A. Nilsson, M. Weinelt, T. Wiell, C. Puglia, N. Wassdahl, N. Martensson, M. Samant, J. Stohr, *Phys. Rev. Lett.* **1996**, *76*, 1380–1383.
- [11] L. C. Duda, T. Schmitt, A. Augustsson, J. Nordgren, *J. Alloys Compd.* **2004**, *362*, 116–123.
- [12] a) P. A. Brühwiler, O. Karis, N. Martensson, *Rev. Mod. Phys.* **2002**, *74*, 703–740; b) C. Monney, K. J. Zhou, H. Cercellier, Z. Vydrova, M. G. Garnier, G. Monney, V. N. Strocov, H. Berger, H. Beck, T. Schmitt, P. Aebi, *Phys. Rev. Lett.* **2012**, *109*, 086401.
- [13] a) L. Triguero, A. Fohlisch, P. Vaterlein, J. Hasselstrom, M. Weinelt, L. G. M. Pettersson, Y. Luo, H. Agren, A. Nilsson, *J. Am. Chem. Soc.* **2000**, *122*, 12310–12316; b) M. Nyberg, A. Fohlisch, L. Triguero, A. Bassan, A. Nilsson, L. G. M. Pettersson, *J. Mol. Struct. THEOCHEM* **2006**, *762*, 123–132; c) J. Gladh, H. Oberg, J. Li, M. P. Ljungberg, A. Matsuda, H. Ogasawara, A. Nilsson, L. G. M. Pettersson, H. Ostrom, *J. Chem. Phys.* **2012**, *136*, 034702–034710; d) A. Nilsson, L. G. M. Pettersson, *Surf. Sci. Rep.* **2004**, *55*, 49–167; e) A. Nilsson, L. G. M. Pettersson, J. K. Nørskov, *Chemical bonding at surfaces and interfaces*, 1.ed., Elsevier, Amsterdam, **2008**.
- [14] P. Skytt, P. Glans, K. Gunnelin, J. H. Guo, J. Nordgren, *Phys. Rev. A* **1997**, *55*, 146–154.